Detecting and Measuring Turbulence from Mode S Surveillance Downlink Data

Olive, Xavier; Sun, J.

Publication date
2020

Document Version
Final published version

Published in
ICRAT 2020

Detecting and Measuring Turbulence from Mode S Surveillance Downlink Data

Xavier Olive
ONERA – DTIS
Université de Toulouse
Toulouse, France

Junzi Sun
Faculty of Aerospace Engineering,
Delft University of Technology,
Delft, the Netherlands

***Abstract*—Instability in the movement of air masses in the atmosphere can result in turbulence. Most often, turbulence causes discomfort to passengers but it can occasionally affect their safety as well. Turbulence experienced by aircraft can be difficult to predict, especially for clear air turbulence (CAT) which occurs in the absence of any visual clues. Pilots may report turbulence when they fly through turbulent areas; their input contributes to the issuance of weather advisories (SIGMETs) that contain meteorological information concerning the safety of all aircraft.**

This paper presents a novel method to detect turbulence experienced by aircraft based on Mode S data, emitted by transponders in reply to BDS 6,0 requests (heading and speed reports) sent by Secondary Surveillance Radars. The method is first validated on a few flights labelled manually by the authors flying around Europe. Then, a large-scale reconstitution of turbulent areas over Europe on ten days across different seasons in 2018 is compared with SIGMETs emitted during the same time interval. This method may be an encouraging entry point for Air Navigation Service Providers so as to gain a better awareness of the turbulence situation, by simply requesting this type of information from aircraft flying in their airspace.

***Keywords*— aircraft trajectory, turbulence, ADS-B, Mode S, data analysis**

I. Introduction

Aircraft experience turbulence as they fly through an area where they are subject to volatile and unsteady movements. Commonly, there are four fundamental causes of turbulence for aircraft, namely thermal, shear, mechanical, and aerodynamic. Thermal causes refer to the formation of vertical air flows due to an increase in surface temperature. Shear causes refer to the fronts where wind directions change drastically within a short range. Mechanical causes refer to the interference of horizontal air flow with obstacles such as mountains and buildings, which causes rising air flow. Finally, aerodynamic causes commonly refer to the wake vortex generated by nearby aircraft.

Turbulence is a weather phenomenon that is difficult to consider during flight planning because of its varying nature. Most of the time, aircraft fly through turbulence without incurring any damage; however, every year there are aircraft that are damaged, passages that are injured or flights that must be diverted to nearby airports due to turbulence. On February 13, 2019, Delta Airlines 5763 from Orange County (Southern California) to Seattle made an emergency landing at Reno Airport after experiencing severe turbulence. On March 9, 2019, Turkish Airlines 1 from Istanbul to New-York JFK experienced severe turbulence above Maine at FL320 and required immediate descent to FL240; approximately 30 passengers and crew were treated for injuries after landing.

Providing better information on turbulence is an essential step to improving air safety. Satellite remote sensing has provided methods to capture certain types of turbulence such as convective or clear air turbulence [1]. Similarly, aircraft may also provide their own information on turbulence with air traffic controllers. Meteorological routine air report (MRAR) and meteorological hazard report (MHR) from Mode S communication are designed to allow this information to be interrogated by Secondary Surveillance Radars (SSR). There are a couple of limitations regarding the current use of Mode S meteorological reports. Firstly, few radars around the world actually emit MRAR and MHR requests [2]. Secondly, few transponders are compliant and reply to such requests. These factors greatly reduce the availability of meteorological reports. However, other types of Mode S messages are more widely and commonly interrogated. Heading and speed reports, for example, are widespread and frequently requested, at least in Europe.

In this paper, we propose a new approach to detect and measure turbulence using aircraft Mode S surveillance data. We use parameters decoded from Mode S heading and speed reports [3] to detect and reconstruct turbulence experienced by aircraft flying in controlled airspaces implementing Mode S requests. The two key parameters used for this research are two different sources for vertical speed: a barometric raw unfiltered measure and a baro-inertial measure computed and filtered by inertial systems. Turbulence is a common source of noise in the barometric measure of altitude: barometric vertical rate is provided unfiltered, turbulence-related noise is amplified. Baro-inertial vertical rate is computed after multi-sensor data fusion: it represents the same physical quantity where noise is filtered. Therefore, we analyse the differences in variance of these two parameters and use it to detect turbulence.

The paper is structured as follows: Section II presents common sources of information related to turbulence and details the standard specifications related to the parameters we take into account. It explains how vertical speed is commonly measured and filtered by inertial systems. Section III presents how we compute indicators relevant to turbulence and formally describes the processing of data. Then, Section IV validates

our approach on single flights, as well as at a global level with situation awareness heat maps calculated above Europe and compared with other sources of information such as SIGMETs and wind fields. Section V concludes and addresses the potential of such a proof of concept.

II. Technical Background

A. Traditional turbulence information

Information about the location of turbulence areas is commonly advertised using SIGMETs, i.e. inflight weather advisories for significant meteorological hazards. A SIGMET is widespread in that it covers an area of at least 3,000 square miles, although the particular hazard may be present in only a small portion of the area at any particular time. SIGMET reports are issued for various hazard types, including thunderstorm (TS), icing (ICE), turbulence (TURB) or volcanic ashes. Turbulence (TURB) reports are only issued if they are not associated with thunderstorms, as those are covered by thunderstorm (TS) reports.

SIGMETs may be issued based on forecasts or observations. Forecasts can be problematic, as they are often vague or of poor accuracy, which leads many pilots to pay little attention to such information. Observations are based on pilot reports of actual weather conditions encountered during flight. This information is usually relayed by radio or electronic submission to the nearest ground station. Pilot reports should contain location, time, intensity, altitude, whether in or near clouds and, if applicable, duration of turbulence.

B. Turbulence in meteorological routine and hazard reports

Meteorological information is sometimes transmitted using Mode S Data Link, through Meteorological Routine Air Report (MRAR) and Meteorological Hazard Report (MHR). In both reports, the severity of the turbulence is indicated. According to Mode S technical standard [4], the turbulence can be reported as one of four levels, which are nil (level 0), light (level 1), moderate (level 2), and severe (level 3).

In a perfect world, Mode S meteorological reports could have been a good source for turbulence: the data is transmitted in real time based on measurements made by the aircraft flight management system. However, a couple of limitations prevent them from being a useful data source on a large scale. First, these messages are only transmitted upon requests of secondary surveillance radars (SSR), and there are currently only few SSR requesting such information in Europe [5]. In addition, since MRAR and MHR capabilities are not a mandatory requirement in the implementation of Mode S transponders, only a small fraction of aircraft have these capabilities enabled [6].

With these limitations in mind, we consider Mode S meteorological reports are not a reliable source of information for studying air traffic related turbulence.

C. Mode S heading and speed report

Mode S communications also provide many other flight parameters including positions, speeds, and altitudes from ADS-B. Our goal is to leverage information contained in Mode S heading and speed reports (BDS 6,0) to infer occurrences of turbulence. In these reports, two different types of vertical movement measurements are transmitted, namely *barometric altitude rate* and *inertial vertical velocity*.

Barometric altitude rates are only derived from barometer measurements. This source of information being unfiltered, significant noise is contained in these values. Inertial vertical velocities are values provided by navigational equipment from different sources including the flight management computer. According to [4], data sources with different level of priorities are defined for these two values, as listed in Table I. Regarding barometric altitude rate, the preferred data source is the Air Data System, which obtains data from aircraft Pitot-static systems. The inertial vertical rate data is primarily provided by the Flight Management Computer, which fuses information from multiple data sources including the Global Navigation Satellite System (GNSS).

TABLE I
Data sources for barometric and inertial vertical rate in Mode S heading and speed report

Parameter	**Input Data Source Priorities**
Barometric altitude rate	1. Air Data System 2. Inertial Reference System / Flight Management System
Inertial vertical rate	1. Flight Management Computer / GNSS integrated 2. Flight Management Computer (General) 3. Inertial Reference System / Flight Management System

D. Estimation of aircraft vertical speed

Aircraft air data systems (or Pitot-static systems) provide input for the vertical speed indicator. Barometric altimeters measure a differential of barometric pressure. The measured altitude $\tilde{h}$ can be decomposed as a sum of three terms: the altitude h, a term for bias induced by the barometric setting b, and noise n_h. Sources of noise in the measurements are many. Specifically, common sources of high frequency noises are:

1) accelerations impacting the capsules forming the altimeter; manufacturers tend to place these capsules vertically in an attempt to alleviate these effects.
2) disrupted airflow during certain maneuvers, phases of flight and wind conditions; disturbed airflow over the static port can cause erroneous readings on the altimeter.

As vertical speed cannot be directly measured by sensors, a first raw estimation can be made by measuring the derivative of barometric altitude in the air data system. The derivative of the barometric altitude is referred to as *barometric altitude rate* (or `vs_barometric`) in the following. This source of information includes the derivative of high frequency noises in the measure of the altitude. High frequencies are amplified by the differential operator.

On the other hand, the onboard flight control computer has inputs from additional sources, such as inertial and GNSS guidance systems. Based on these multiple inputs, including (inertial) accelerometer and (barometric) altimeter, sensor

fusion is performed. Extended Kalman Filters (EKF) are a common option to provide a better estimation of the vertical speed [7] than by either integrating inertial accelerations or differentiating barometric altitudes. With sensor fusion, noise is filtered in the final estimation. The output of this fusion method is referred to as *inertial vertical rate* (or `vs_inertial`) in the following.

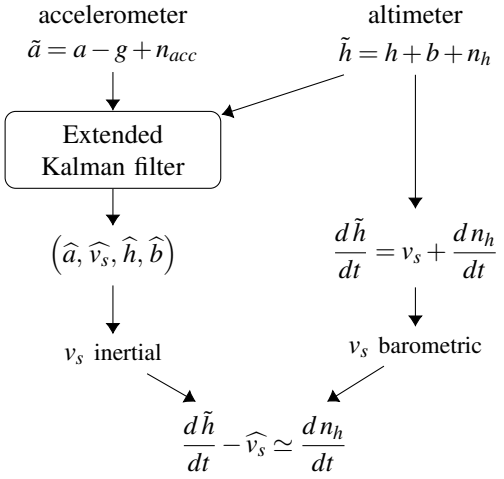

Fig. 1. If we subtract the two estimations of v_r we get a good estimate of high frequency noise impacting the altimeter

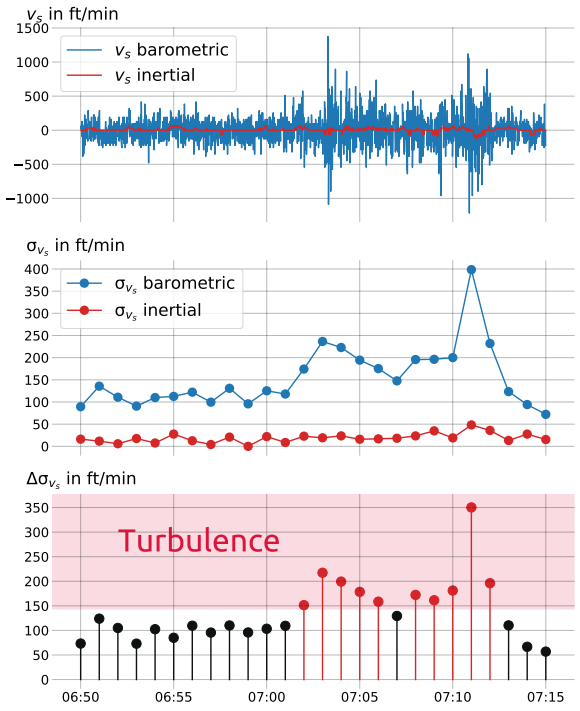

Fig. 2. Standard deviations in two types of vertical rate values, with windows size of 60 seconds and corresponding detected turbulence areas.

The methodology presented in this paper is depicted in Figure 1; it is based on the difference between the two sources of vertical rate, namely the filtered baro-inertial measurements and the raw barometric measurements. We find that this measure, a differential of high frequency noise, is a good indicator of the turbulence experienced by the aircraft.

III. Methodology

A. Turbulence detection using Mode S data

The difference between barometric and inertial vertical speeds appears clearly in flight data. Figure 2 (top) plots both barometric and inertial vertical speed signals as received in BDS 6,0 reports for an example flight during cruise. As expected, the barometric signal is more noisy than the inertial one. It also appears that noise in the barometric signal varies over time. We observe that aircraft flying through a turbulence area will see more noise in their barometric altitude rate.

A basic way to detect volatility in a time series is to calculate the standard deviation of the values within small time segments. With sliding windows (we chose one minute intervals), we calculate the variations in both barometric altitude rate and inertial vertical rate in heading and speed reports and plot it in Figure 2 (middle).

During en route phase, the standard deviation computed on sliding windows with the barometric altitude rate signal would be sufficient to detect turbulence. In order to address climb and descent phases as well, we look in Figure 2 (bottom) at the difference between the slided standard deviation values of both barometric and inertial measurements.

However, noise patterns are not similar across different types of aircraft and transponders. Noise in Figures 5 and 6 follows a different pattern. Figure 3 shows four full trajectories with their distributions of $\Delta\sigma_{v_s}$, which can look simply exponential or display the constant low noise present during the cruise phase for some aircraft.

For illustration purposes, we set the thresholds manually in Figure 2, 5 and 6 and discuss the impact the threshold determination in Section IV-A. For a systematic approach on large-scale data, we come to the following threshold:

$$\Delta\sigma_{v_s} \geq \overline{\Delta\sigma_{v_s}} + 1.2 \cdot \sigma\left(\Delta\sigma_{v_s}\right) \tag{1}$$

where $\overline{\Delta\sigma_{v_s}}$ is the average of standard deviation difference during the flight and $\sigma\left(\Delta\sigma_{v_s}\right)$ is the standard deviation of $\Delta\sigma_{v_s}$ over the entire flight. This equation can be interpreted as a value of $\Delta\sigma_{v_s}$ clearly above average. Figure 3 shows how the threshold impacts the detection of turbulence with various noise profiles.

B. Description of the data preprocessing

We use the declarative processing grammar from the Python traffic [8] library (version 2.3) to describe the preprocessing applied to our data set of trajectories. The main steps include (implicitly) iterating over a set of trajectories, applying median filters on each trajectory in order to remove obviously abnormal data, aggregating the standard deviation of two measures of vertical speeds over a defined time interval, and calculating a quantified indicator called `criterion` that corresponds to $\Delta\sigma_{v_s}$. We use this criterion to detect and label turbulence.

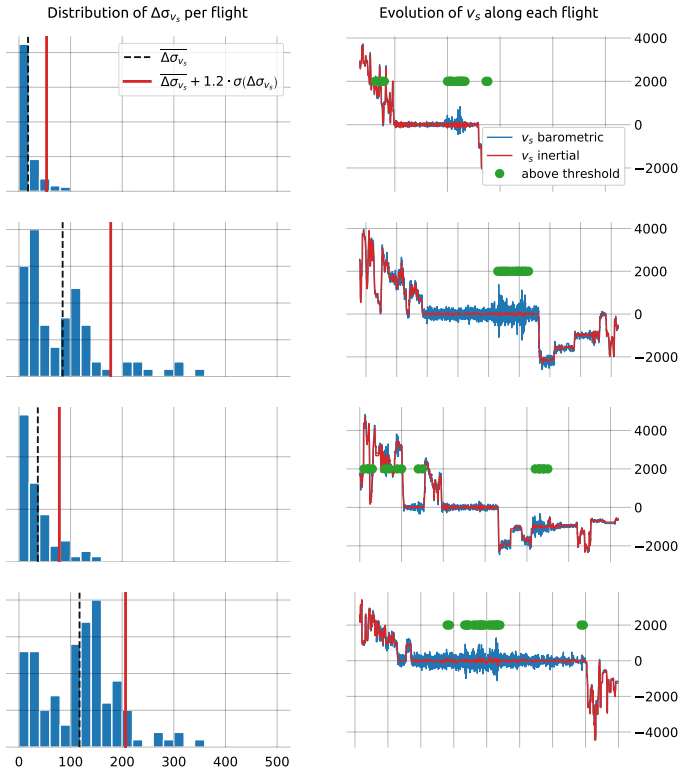

Fig. 3. All aircraft (and transponders) do not display the same noise patterns. Eq. (1) yields a reasonable threshold for all patterns we manually encountered.

```
original_data
.filter(  # median filters for abnormal points
    barometric=3, inertial=3,  # kernel sizes
    strategy=None,  # invalid data becomes NaN
)
.agg_time(
    # aggregate data over intervals of one minute
    "1 min",
    # compute the std of the data
    inertial="std", barometric="std",
    # reduce one minute to one point
    latitude="mean", longitude="mean",
)
.assign(
    # we define a criterion based on the
    #  difference between two standard deviations
    #  on windows of one minute
    criterion=lambda df:
        (df.barometric_std-df.inertial_std).abs()
)
.eval()  # triggers iteration, evaluation and reduce
```

IV. Results

A. Validation on single flights

A first validation of the presented approach is conducted based on flights boarded by the authors. We present here three specific flights from Toulouse chosen for the diversity of situations they display. Clock synchronisation issues being unavoidable, we wrote down timestamps using an `HH:MM` format as displayed on personal watches; each timestamp is associated to turbulence experienced. As a consequence, we plot in Figures 5 and 6 one-minute intervals of experienced turbulence using bars appended on a new axis at the bottom of each plot.

Intensity of turbulence for most travellers is a very subjective, idea and two passengers in the same aircraft will not experience the same level of discomfort when they fly through turbulence. As a consequence, we consider potential annotations of severity of turbulence irrelevant for this kind of naive validation.

Fig. 4. Flight `DLH07F` from Toulouse to Frankfurt on November 15th 2018. The author experienced turbulence above Switzerland. Weather was overcast at low altitude only, so we suspect the influence of Alps mountains.

Figure 5 shows a clear correlation between our indicator and experienced turbulence. Although we do not have enough elements to interpret it, we suspect the influence of the Alps mountains on the first time interval labelled with turbulence.

Figure 6 plots some light turbulence experienced during the end of climb, corresponding with the crossing of the Pyrenees mountains, although their detection would depend on how the threshold is set. Stronger turbulence was later experienced; the authors noted the seat belt sign was on before the stronger turbulence, suggesting that turbulence areas were identified before we flew through them.

B. Large-scale analyses

We implemented the detection method described in this contribution on 7 days of traffic above Europe and across seasons, every 50 days, i.e. Jan 1st, Feb 19th, Apr 10th, May 30th, Jul 19th, Sep 7th, Oct 27th and Dec 16th 2018. ADS-B data above a large bounding box covering the European continent (25°W–55°E and 32–65°N) and associated Enhanced Mode S raw messages were downloaded from the OpenSky Network database [9] and decoded using pyModeS Python library [3]. One day worth of resulting data represents between 5 and 10 Gb of binary data depending on the coverage on each specific day. The chosen approach is to cross-check different sources of data. In particular, we attempt to show that:

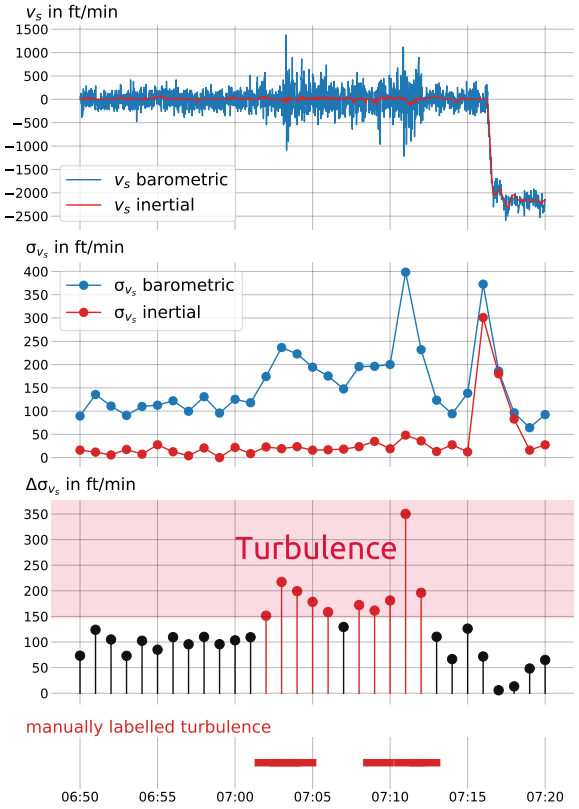

Fig. 5. Flight DLH07F from Toulouse to Frankfurt on November 15th 2018.

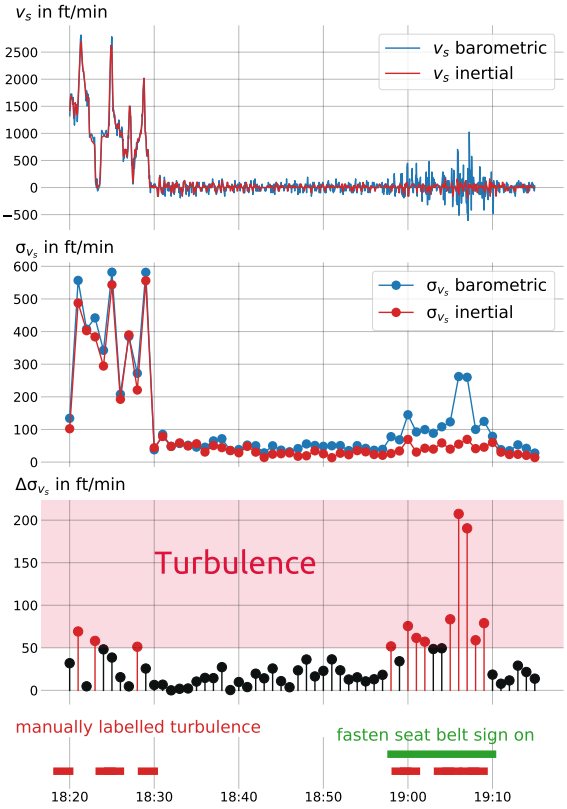

Fig. 6. Flight TAP499 from Toulouse to Lisbon on November 26th 2018. Influence of relief is clear when the aircraft crosses the Pyrenees mountains.

- severe turbulence is consistently observed by all aircraft flying through the same area;
- turbulence evolution over time is consistent;
- detected turbulence areas match the SIGMETs emitted on that day for that area;
- detected shear turbulence when crossing particular flight levels in terminal maneuvering areas is consistent with reconstructed wind fields.

1) Consistency across aircraft: In this subsection, we demonstrate the geographical consistency of observed turbulence across trajectories. For this specific purpose, we reduce our analysis to a smaller bounding box above Southern Germany and Switzerland. Figure 7 (left) plots all the trajectories above 20,000 ft crossing the bounding box (7–10°E and 47–50°N) between 20:00 and 20:30 UTC. The red part highlights the segments of trajectories when each aircraft experienced turbulence ($\Delta\sigma_{v_s}$ above threshold).

The first striking observation is that aircraft do not fly through some parts of the map: we cannot record any observations in these areas. Looking at the situation on a larger scale, aircraft seem to deliberately avoid these areas, most likely because of a thunderstorm activity.

However, the location of observed turbulence looks consistent on each flow of trajectories. Few trajectories crossing this North–South cluster experience turbulence at consistent locations. For the sake of legibility, we produce heat maps on Figure 7 (right), based on the average of our $\Delta\sigma_{v_s}$ criterion presented in Section III across all trajectories overlaying each grid cell. In the following, we also filter out cells where only one aircraft experienced turbulence. We argue that this kind of map offers a convenient reading grid and provides awareness of the location and severity of turbulence in the area.

2) Consistency over time: Next, we demonstrate the temporal consistency of observed turbulence over time. Figure 8 plots turbulence over a large area, roughly corresponding to the area controlled by MUAC center. Four snapshots are made between 11:00 and 13:00 UTC, with trajectories flying in the next 30 minutes. Positions of four major airports are provided as a visual reference, being helpful for comparing the snapshots.

The plots demonstrate a clear consistency along time: areas consistently impacted are the Benelux area, more specifically Flanders and the Netherlands, Groningen province to the North-East of the country being relatively spared, and, to a lesser extent, the North and the East of Paris. Meanwhile, Western Germany and Great Britain are quite free of turbulence during the observation period.

3) Consistency with SIGMET reports: In the following, we compare the geographical footprints of turbulence that have been detected with the method presented in this contribution and weather advisory (SIGMET) reports issued for the same time intervals. In this section, we consider both TS (thunder-

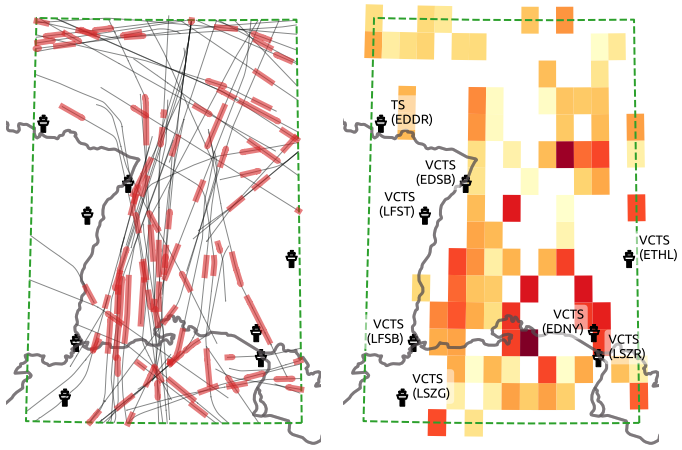

Fig. 7. Turbulence observed over Baden-Württemberg (Southern Germany) and Northern Switzerland on May 30th 2018. On the left map, observed turbulence looks consistent across trajectories; a heat map is then computed and printed on the right hand side. Local airports are displayed with their current METAR as a visual reference when comparing the snapshots.

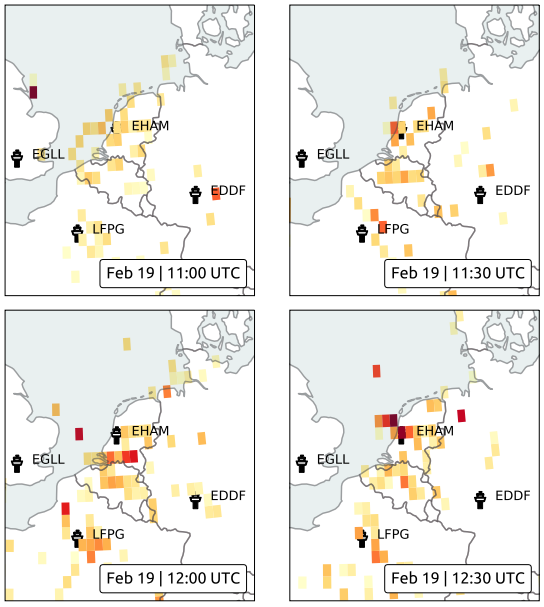

Fig. 8. Turbulence detected over an extended area on February 19th. Snapshots produced every 30 minutes show consistent locations of turbulence over time. Major airports are displayed as a visual reference when comparing the snapshots.

storm) and TURB (turbulence) reports, as turbulence due to thunderstorm activities will not trigger a TURB report if a TS report has been issued.

Figure 9 plots the situation in the Northwestern quarter of France on July 19th, 2018 around 18:00 UTC. Three TS SIGMET forecast reports were filed simultaneously for the corresponding Flight Information Region (FIR) for the two hours to come. The timestamps remind that the same authority (LFPW) issued the three polygons, which spectacularly match the area of detected turbulence.

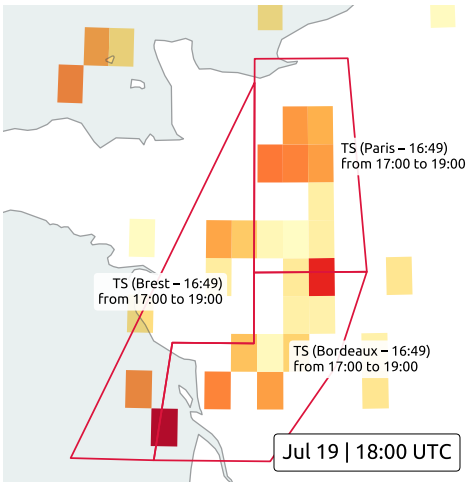

Fig. 9. Turbulence detected over Northwestern France on July 19th 2018, 18:00 UTC, perfectly matching TS (thunderstorm) SIGMET forecast reports issued on three Flight Information Regions (FIR) in France.

Figure 10 represents the joint evolution of detected turbulence and SIGMET forecast reports in Northern Italy (Milano FIR) on December 16th, 2018. The top-left quadrant plots the situation between 10:30 and 11:00 UTC, where we see that the SIGMET polygon only poorly matches the turbulence area. Only the seaside area is affected, meaning the Northern part of the polygon is unnecessarily affected by the SIGMET. Conversely, the area to the East of the polygon is clearly affected by turbulence but not reported as so.

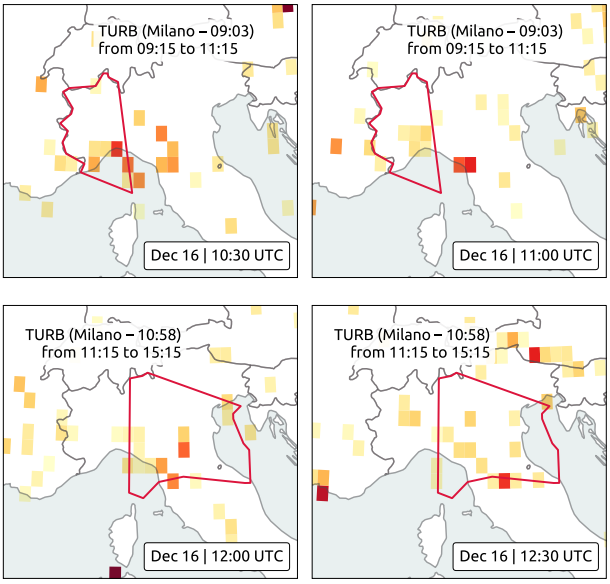

Fig. 10. Turbulence detected over Northern Italy on December 16th, 2018. It should be noted that the SIGMET forecast on the East side of Milano FIR has been issued at 10:58 UTC, after we detected turbulence around 10:30 UTC.

The geographical footprint of the forecast turbulence is updated at 10:58 UTC for four hours starting at 11:15 UTC. The observed evolution over the following hour is consistent

with the new SIGMET. This figure suggests that a possible extension of the contribution into an automatic system to label turbulence areas would probably have drawn different, yet consistent polygons associate with turbulence events.

Figure 11 shows an interesting pattern of cross-border turbulence above four countries (Belgium, France, Germany and Luxembourg) and four FIRs (Brussels, Langen, Paris and Reims). Here, it appears that three systems forecast turbulence and issue SIGMET reports asynchronously: first Langen forecast turbulence on a 80nm wide line on their side of the border. Then, French FIRs (Paris and Reims) file SIGMET reports on an overestimated polygon, followed by Belgium issuing a SIGMET report covering half the country when only Luxembourg seemed affected.

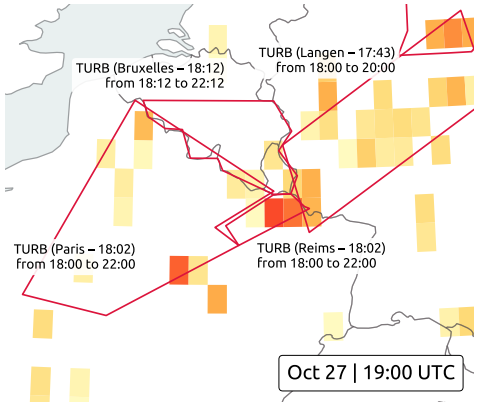

Fig. 11. Turbulence detected on October 27th, 2018, at the border of four countries (also four FIRs). Brussels and Paris seem to overestimate the geographical location of turbulence.

Lastly, Figure 12 over the Balkans on July 19th 2018 looks intriguing. Bulgaria, Serbia and Romania were impacted by turbulence for the whole day, yet no turbulence SIGMET reports have been issued by any country. Bucharest in Romania issued TS SIGMET observation reports for the Northern part but missed the turbulence in the Southwestern part of the country.

4) Consistency with wind fields: When we analyse data over London on October 27th, it appears that only aircraft evolving vertically, i.e. landing at or taking off from London are subject to turbulence. Figure 13 plots the vertical distribution of turbulence above London on that day. In this figure, the x-axis indicates the time, and color is associated with the strength of our criterion. A clear pattern occurs between 14:45 and 15:00 UTC where aircraft flying between 10,000 and 20,000 ft are subject to possibly strong turbulence.

Accurate high-resolution wind fields can be constructed based on ADS-B and Mode S Enhanced Surveillance data. Using the Meteo-Particle model presented in [10], ground speed, airspeed, track angle and heading information broadcast by different aircraft are combined and used to reconstruct the wind field. In this demonstration, we construct a wind field over a large area covering Southern England at the time when turbulence is detected.

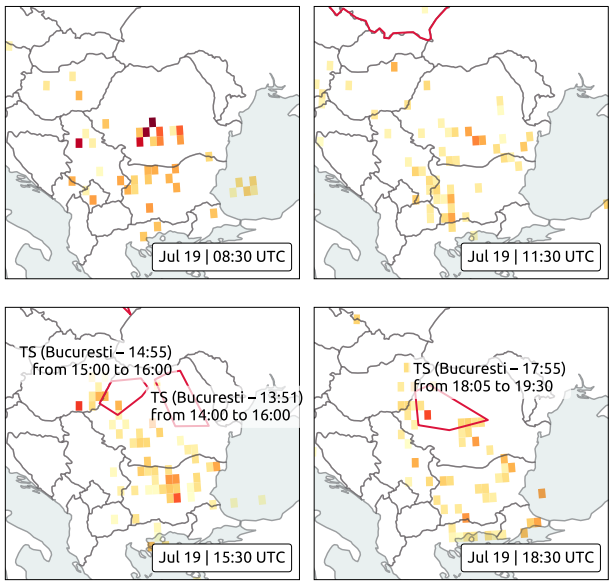

Fig. 12. Turbulence detected on July 19th, 2018. We found temporal consistency all day for turbulence on Bulgaria and the Southern part of Romania. Only Bucharest issued some TS SIGMET observation reports but these geographical footprints for thunderstorm activities seem to miss the area of turbulence.

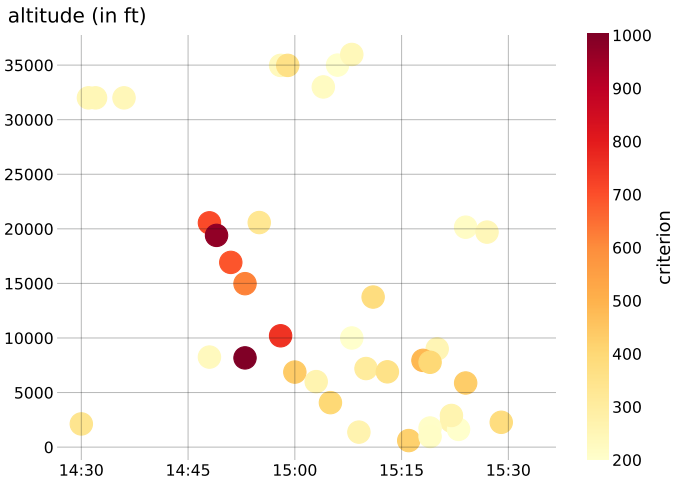

Fig. 13. Most turbulence detected above the Greater London area occurs between 10,000 and 20,000 ft.

Figure 14 plots wind fields reconstructed from Mode S data during that time interval, at different levels between 10,000 and 25,000 ft, together with an aggregated heat map of turbulence areas observed below 25,000 ft. A swirling structure of wind movements above London at higher altitudes (see 25,000 ft) appears with winds flowing southbound on the Western side of London and northbound on the Eastern side of London. Near the surface, the wind movement is different and consistently rather southbound. As a consequence, aircraft flying down to one of London airports (mostly Heathrow) from the Eastern side of the city must cross altitude layers where wind turns from a northbound to a southbound direction.

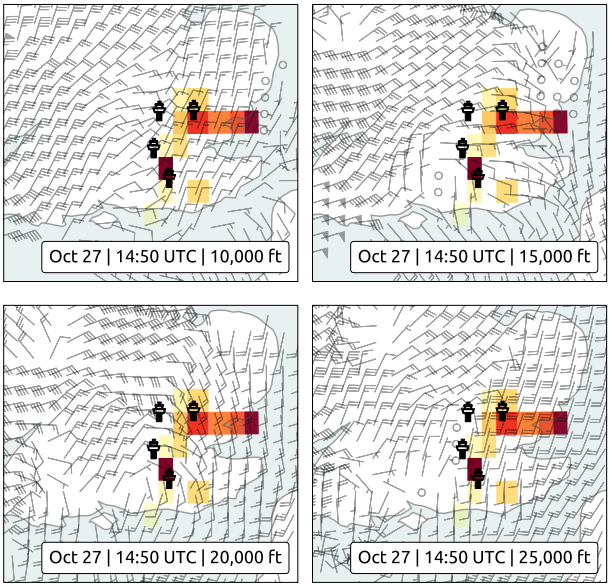

Fig. 14. Turbulence detected based on aircraft landing in any of the four London airports (Heathrow, Gatwick, Stansted, Luton), with wind barbs at different altitudes.

In such areas, aircraft are indeed subject to turbulence, as mentioned in Section I under the *shear turbulence* category. As a reference, the METAR report in London Heathrow mentions light rain in the area but no particular thunderstorm activity.

V. Conclusions and Future Works

Turbulence is a weather phenomenon with a significant impact on aviation. Detecting and reporting such events can be crucial to improving ATM safety. This paper presents a novel method to detect and reconstruct turbulence maps based on Enhanced Mode S data, specifically heading and speed report (BDS 6,0) messages. The core idea behind this turbulence detection method is to compare variations in vertical speeds provided by both barometric and baro-inertial systems.

Heading and speed reports are consistently requested across Europe. It is common to have one sample per radar sweep per aircraft. Due to the overlapping of many Secondary Surveillance radars, update intervals can be higher. The large amount of Mode S messages gathered by an open crowd-sourced receiver network – The OpenSky Network – provides us sufficient data to challenge our turbulence detection method.

First, we validated our solution with manual labelling based on data and turbulence recorded on board. Then, in order to further corroborate the detection method, several follow-on demonstrations were conducted; we examined the consistency of turbulence spatially and temporally, compared specific turbulence situations with SIGMET reports, and validated the detection of shear turbulence based on reconstructed wind fields. We argue that reconstructed turbulence based on our method could complement and provide assistance in issuing SIGMET reports in the future.

The proposed method is not without its own limitations. It can only be applied to areas where aircraft are flying since aircraft are the sensors. The detection method also relies on the reception of Enhanced Mode S reports. These reports are common in Europe but are not always requested in other airspace, including most of the United States or over the oceans.

Future works would include real-time detection of turbulence, improvements in short-term predictions, investigation of the effects on possible rerouting options, and further validation with space-based turbulence detection and prediction. This work, once taken past the proof of concept, could result in recommendations to further implement Enhanced Mode S and to consistently request heading and speed reports in any area subject to severe turbulence.

Acknowledgements

The authors wish to thank Philippe Mouyon from ONERA for sharing his expertise in sensor fusion and onboard measurement systems and Maxime Warnier from MetSafe ATM for his help in parsing SIGMET archives and sharing them in structured familiar formats.

References

[1] S. R. Proud, “Analysis of aircraft flights near convective weather over Europe,” *Weather*, vol. 70, no. 10, pp. 292–296, Oct. 2015. [Online]. Available: http://doi.wiley.com/10.1002/wea.2569

[2] J. Sun and J. M. Hoekstra, “Integrating pyModeS and OpenSky Historical Database,” in *Proceedings of the 7th OpenSky Workshop*, vol. 67, 2019, pp. 63–72.

[3] J. Sun, H. Vû, J. Ellerbroek, and J. M. Hoekstra, “pyModeS: Decoding Mode-S Surveillance Data for Open Air Transportation Research,” *IEEE Transactions on Intelligent Transportation Systems*, 2019.

[4] ICAO, “Manual on Mode S Specific Services, 2nd Edition,” Tech. Rep. Doc 9688, AN/952, 2004.

[5] S. de Haan, “Availability and quality of Mode-S MRAR (BDS4.4) in the MUAC area: a first study,” *KNMI, the Netherlands*, pp. 2014–01, 2014.

[6] B. Strajnar, “Validation of Mode-S meteorological routine air report aircraft observations,” *Journal of Geophysical Research: Atmospheres*, vol. 117, no. D23, 2012.

[7] A. Sabatini and V. Genovese, “A Sensor Fusion Method for Tracking Vertical Velocity and Height Based on Inertial and Barometric Altimeter Measurements,” *Sensors*, vol. 14, no. 8, pp. 13 324–13 347, Jul. 2014. [Online]. Available: http://www.mdpi.com/1424-8220/14/8/13324

[8] X. Olive, “traffic, a toolbox for processing and analysing air traffic data,” *Journal of Open Source Software*, vol. 4, no. 39, p. 1518, Jul. 2019. [Online]. Available: http://joss.theoj.org/papers/10.21105/joss.01518

[9] M. Schäfer, M. Strohmeier, V. Lenders, I. Martinovic, and M. Wilhelm, “Bringing up OpenSky: A large-scale ADS-B sensor network for research,” in *Proceedings of the 13th international symposium on Information processing in sensor networks*, 2014, pp. 83–94.

[10] J. Sun, H. Vû, J. Ellerbroek, and J. Hoekstra, “Weather field reconstruction using aircraft surveillance data and a novel meteo-particle model,” *PLoS ONE*, vol. 13, no. 10, 2018.